RESEARCH REPORT

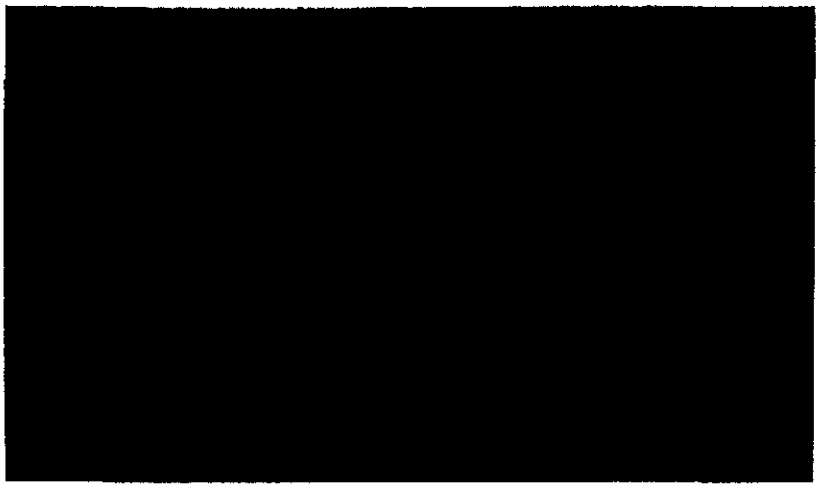

Battelle

Columbus Laboratories

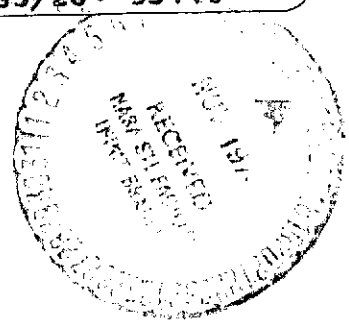

BATTELLE'S COLUMBUS LABORATORIES comprises the original research center of an international organization devoted to research and development.

Battelle is frequently described as a "bridge" between science and industry – a role it has performed in more than 90 countries. It conducts research encompassing virtually all facets of science and its application. It also undertakes programs in fundamental research and education.

Battelle-Columbus – with its staff of 2500 -- serves industry and government through contract research. It pursues:

- research embracing the physical and life sciences, engineering, and selected social sciences
- design and development of materials, products, processes, and systems
- information analysis, socioeconomic and technical economic studies, and management planning research.

505 KING AVENUE • COLUMBUS, OHIO 43201

FINAL REPORT

on

SINGLE CRYSTALS OF METAL SOLID SOLUTIONS

to

NATIONAL AERONAUTICS AND SPACE ADMINISTRATION
GEORGE C. MARSHALL SPACE FLIGHT CENTER

September 3, 1974

by

J. F. Miller, A. E. Austin, N. Richard, N. M. Griesenauer,
D. P. Moak, M. R. Mehrabian, and S. H. Gelles

Contract No. NAS8-29875
NASA Control No. PR-R-29875

Covering the Period October 9, 1973, to August 30, 1974

BATTELLE
Columbus Laboratories
505 King Avenue
Columbus, Ohio 43201

This report was prepared by Battelle's Columbus Laboratories under NASA Contract No. NAS8-29875 entitled "Single Crystals of Metal Solid Solutions" for the George C. Marshall Space Flight Center of the National Aeronautics and Space Administration.

TABLE OF CONTENTS

TABLE OF CONTENTS
(Continued)

LIST OF TABLES

LIST OF FIGURES

LIST OF FIGURES
(Continued)

FINAL REPORT

on

SINGLE CRYSTALS OF METAL SOLID SOLUTIONS

to

NATIONAL AERONAUTICS AND SPACE ADMINISTRATION
GEORGE C. MARSHALL SPACE FLIGHT CENTER

from

BATTELLE
Columbus Laboratories

by

J. F. Miller, A. E. Austin, N. Richard, N. M. Grisenauer,
D. P. Moak, M. R. Mehrabian, and S. H. Gelles

September 3, 1974

INTRODUCTION

The growth of high-quality homogeneous crystals of metal solid solutions requires that primary consideration be given to two key factors that can produce deleterious substructures in the solid-solution crystals: (1) constitutional supercooling, which produces cellular growth composed of cells defined by compositional variations that are elongated in the growth direction, and (2) growth heterogeneities resulting from temperature fluctuations at the solid-liquid interface that produce compositional variations in the form of bands perpendicular to the growth direction. Constitutional supercooling can be controlled by altering the interfacial growth conditions, growth rate, and temperature gradient. However, temperature fluctuations which produce compositional banding during crystal growth result from convection occurring in the liquid ahead of the advancing solid interface. This convection, which is gravity driven, is increased by imposing greater temperature gradients designed to eliminate cellular growth. The convection currents cannot be entirely eliminated in terrestrial processing in a gravity field. Thus, investigating alloy crystal growth and solidification in the space-processing development program is amply justified.

This program was designed as a basic study of the effects of convection, gravity, and convection-arresting magnetic fields on the growth of metal solid solution single crystals.

SUMMARY

Objectives

The objectives of the program were

(1) To define the influence of convection and/or gravity present during crystallization on the substructure of a metal solid solution

(2) To define the influence of a magnetic field applied during crystallization on the substructure of a metal solid solution

(3) To define requirements for a space flight experiment to verify results of this study.

Approach

For descriptive and organizational purposes, the program designed to accomplish these objectives was broken down into four tasks, which are briefly described below.

Task I. Investigation of the Influence of Convection on Crystal Growth

This task was conducted to characterize the role of gravity and/or convection during the growth of single crystals of metal solid solutions of αAg-20 atomic percent Zn alloy. The study consisted of the growth of crystals under different combinations of growth rate and temperature gradient conditions. The Bridgman technique and, specifically, normal-freeze crystallization were employed for the crystal-growth experiments. Convective flow behavior during crystal growth was investigated by use of fine-gauge thermocouples placed in the liquid metal. The effects of these variables on crystal growth and substructure of the alloy crystals were investigated under Task III.

Task II. Investigation of the Influence of Magnetic Fields on Crystal Growth

The objective of this task was to determine the influence of magnetic fields on the crystal growth and substructure of solid-solution crystals of αAg-20Zn alloy. Experiments similar to those conducted in Task I were conducted in the presence of transverse magnetic fields (i.e., applied transverse to the direction of crystal growth) of strengths between 50 and 4000 gauss. The effects of the applied magnetic field were investigated under Task III.

Task III. Characterization of Crystals and Analysis of the Effects of Growth Conditions

The objective of this task was to analyze compositional and structural features of the experimental solid-solution crystals grown in Tasks I and II. The crystals were characterized metallographically and by electron microprobe and X-ray diffraction analysis. The results were analyzed with respect to the role of growth conditions--such as growth rate, temperature gradient, and applied magnetic field on the macro- and microstructure of the resulting crystals.

Task IV. Space Flight Experiment Definition

The objective of this task was to provide NASA-MSFC with the information and experimental parameter data required to define a space flight experiment on alloy crystallization or crystal growth if warranted. Experimental results obtained in this program were used as a basis for recommendations regarding a flight experiment on crystallization of metal solid-solution alloy.

Summary of Results

Investigation of Convection Currents

In experiments on determination of the characteristics and effects of convection currents in molten Ag-20Zn alloy in a horizontal boat, temperature fluctuations (resulting from the convection currents) were monitored as overall longitudinal temperature gradients of 1.5, 2.5, 5.5, 7.5, 8, 12, and 16.5 C/cm were imposed in the region of the thermocouples. No significant short-term temperature fluctuations (i.e., periods < 30 seconds) were observed with longitudinal temperature gradients < 8 C/cm.

With overall longitudinal temperature gradients of 12 and 16.5 C/cm, significant short-term temperature fluctuations were observed. Typically, these appeared to be a combination of two or more oscillations having different frequencies, with the result that amplitude peaks varied in magnitude as the oscillations reinforced or opposed one another. Maximum amplitudes (peak to peak) observed were in the range of 0.02 to 0.06 mv ($\sim$ 0.5 to 1.4 C) and periods of the short-term oscillations were observed to be in the range of 6 to 10 seconds. With the exception of a threshold gradient for the onset of short-term temperature fluctuations, no direct relationship between the magnitude of the imposed temperature gradient and the amplitude or period of the temperature oscillations was apparent for the ranges investigated.

Investigation of the Effects of Magnetic Fields

Investigation was made of the effect of applied magnetic fields in the range of 50 to 4000 gauss on convection currents in the molten Ag-Zn alloy held in various temperature gradients.

Low to moderate magnetic fields, i.e., 50 to 250 gauss, decreased the amplitude of convection-current-induced temperature oscillations and damped out some of the complex oscillations, while fields in

the range of 300-350 gauss appeared to damp out all oscillations caused by turbulent convection.

No additional effect was detected when higher magnetic fields (up to 4000 gauss) were applied.

Crystal Growth

Pertinent fluid and diffusional parameters and composition-temperature (i.e., phase stability) data for the Ag-Zn alloy either obtained from the literature or estimated were used to calculate the ranges of experimental conditions that were to be investigated. For the Ag-20Zn alloy at 800 C, the boundary condition for a stable plane interface was estimated to be $G/R > 2 \times 10^5$ C-sec/cm^2, where G is the temperature gradient and R is the growth rate. A crystal growth apparatus with which the required ranges of experimental conditions could be obtained in a magnetic field was designed and built.

A number of horizontal Bridgman crystallization runs were made with and without seeds under conditions calculated to produce constitutional supercooling and cellular growth (i.e., $G/R < 2 \times 10^5$ C-sec/cm^2) and under conditions calculated to give planar interface growth and banding (i.e., $G/R > 2 \times 10^5$ C-sec/cm^2). The single crystal seed material of the Ag-20Zn alloy had been grown in vertical Bridgman growth runs.

In addition, sections of the seeded runs were grown with and without applied transverse magnetic fields of various strengths. This was part of a designed matrix of experiments in which four different growth zones were produced in each run:

(1) Seeding and initial growth

(2) Controlled growth, Zone II

(3) Controlled growth, Zone III

(4) The quenched zone of rapid terminal growth.

From run to run, conditions were varied in each growth zone, particularly with respect to applied magnetic field, which was set in each zone at levels of 0, 400 or 500, 1500, or 4000 gauss. In the final quenched zone, dendritic growth under varied conditions was obtained for study.

Characterization and Analysis

Examination of ingots crystallized under conditions calculated to give constitutional supercooling revealed the expected cellular growth. The results of electron microprobe analyses of the cellular structure indicated that cell-wall thickness and composition differ from ingot to ingot, presumably due to differences in crystallization rate and melt composition. Photomicrographs indicate a modification of the cellular structure due to annealing of the solidified material in the growth furnace during the growth process; this effect, however, has not been confirmed.

Metallographic examination of some ingots grown under conditions calculated to give planar interface growth, both with and without magnetic fields up to 4000 gauss, revealed no unusual microstructural features. However, distinct changes in macrostructure were found to correlate with the application and removal of the magnetic field. For example, growth was polycrystalline (several large crystals) in the absence of the magnetic field but became monocrystalline in regions grown in the magnetic field. Limited X-ray Laue diffraction analysis work conducted on one of the ingots containing alternating sections grown with and without a magnet field indicated that there is a preferred growth direction in both the single-crystal and polycrystalline portions (growth axis approximately parallel with <100>). The two single-crystal portions examined had almost exactly the same orientation. In addition, it was observed in some cases that crystal boundaries formed in a 4000-gauss magnetic field were curved and undulating, whereas boundaries grown in the same ingot in the absence of a magnetic field were planar.

Compositional banding, which was initially expected in this system, was not observed because compositional variations produced during crystallization either were too small to be detected or were reduced below detection limits by the combination of small interband spacing and rapid postgrowth solid state diffusion.

Study of variations in the dendritic growth of the terminal rapid-growth region revealed that there is an effect of magnetic field

on the dendritic growth. With a magnetic field applied (1500-4000 gauss), the dendrites are finer and tend to be preferentially aligned parallel with the ingot-growth axis.

Conclusions and Recommendations

The following conclusions can be made on the basis of this study:

(1) Turbulent convection currents have been detected in Ag-20Zn baths subjected to longitudinal temperature gradients > 12 C/cm.

(2) These convection currents are completely damped by application of moderate magnetic fields (> 300 gauss).

(3) Cellular growth has been observed under the growth conditions $G/R < \sim 2 \times 10^5$ C sec/cm^2, the approximate theoretical threshold value for the cellular planar-interface solidification mode. Electron microbeam probe analysis revealed a cell wall enrichment of between 3 and 9 atomic percent and cell wall thicknesses between 25 and 120 microns.

(4) No evidence of banding was observed in crystals grown under planar interface growth conditions due to the small band spacing expected and the rapid diffusion rate in the solid.

(5) The alternate application and removal of a magnetic field during directional solidification under planar interface conditions demonstrated that growth tended to be polycrystalline without the magnetic field but monocrystalline with it. Laue X-ray diffraction analysis has revealed that there is a preferred growth direction (<100>) under these conditions.

(6) Study of dendritic growth has shown that the application of a magnetic field produces finer

dendrites which are more highly aligned in the growth direction than those produced in the absence of a magnetic field.

The following are recommendations for further work in the area of solid-solution crystal growth:

(1) Studies of the effect of a magnetic field on the morphology and orientation of Ag-Zn crystals grown under planar interface conditions.

(2) X-ray topography and transmission electron microscopy studies of the substructure in Ag-Zn crystals grown under various conditions.

(3) Comparison of the morphology and substructure of Ag-Zn crystals grown under planar interface conditions (with and without a magnetic field) with those grown at 0 g.

(4) Studies of dendrite formation in Ag-Zn alloys grown with and without an applied magnetic field at 1 g and 0 g.

(5) Characterization of Ag-20Zn crystals grown under planar interface conditions in a steep temperature gradient. This will allow the observations of structures which are produced under conditions which are unambiguously planar. It might also allow the use of growth rates which are high enough to produce detectable bands. Modification of the existing equipment would be necessary to carry out this task.

(6) Studies of banding in solid-solution systems having lower solid-state diffusion rates than in the Ag-Zn system, so that band observation is more feasible. Studies in this area should include a comparison of crystals grown without turbulent convection currents, which have been eliminated by either the application of magnetic fields or by a gravitation-free environment.

TECHNICAL AND EXPERIMENTAL DETAILS

Analysis of the Problem

In attempting the growth of high-quality homogeneous crystals of metal solid solutions, primary consideration must be given to two key factors that can produce deleterious substructure in the solid-solution crystals: (1) constitutional supercooling[(1)]*, which produces cellular growth composed of cells defined by compositional variations that are elongated in the growth direction, and (2) growth heterogeneities resulting from temperature fluctuations at the solid-liquid interface which produce compositional variations in the form of bands perpendicular to the growth direction[(2,3)].

Basic heat-flow considerations show that thermal gradients can be controlled independent of growth velocity. This is an important attribute of single-crystal growing furnaces, since growing good crystals of metal solid solutions requires that the temperature gradients be high and the growth rate be low.

Constitutional supercooling is produced under certain growth-rate and temperature-gradient conditions. Quantitatively, the general constitutional supercooling criterion for a stable plane front interface requires that the ratio of the temperature gradient in the liquid, G_L, to the crystallization rate, R, be

$$\frac{G_L}{R} \geq -\frac{m_L C_s^* (1-k)}{kD_L} \quad , \tag{1}$$

where

m_L = slope of the liquidus line

C_s^* = composition of the solid forming at the liquid-solid interface

k = equilibrium partition coefficient $\sim C_s^*/C_L^*$

D_L = diffusion coefficient of solute in the liquid.

This criterion, then, establishes the critical or maximum growth rate and the critical or minimum temperature gradient to sustain plane front growth.

---

* References are listed on Page 46.

Solute distribution in the liquid ahead of the liquid-solid interface is an important factor affecting crystal perfection. It is diffusion controlled but is also affected by convection in the liquid. Solidification of a metal solid solution from the melt can be closely approximated by the assumption of equilibrium at the interface during growth. There may be large concentration gradients in the solid and the liquid during solidification, but there is only a negligible barrier to transport of atoms across the interface. Condition of equilibrium at the liquid-solid interface where solidification is occurring at a given temperature requires that the liquid and solid compositions at the interface be given by the phase diagram relationship.

An "equilibrium partition ratio", k, can be defined as the ratio of the concentration of the solute element in the solid and the liquid at the interface, i.e.,

$$k = \frac{C_S^*}{C_L^*} \quad . \tag{2}$$

The quantitative treatment of solute distribution to be given employs the further assumption of no significant undercooling at the interface before nucleation or from the effect of radius of curvature. A quantitative treatment of solute distribution should also take convection in the liquid into consideration.

Solidification and growth in the absence and presence of convection must be considered in the treatment of solute distribution and its effect on substructure in the growing crystal. Let us consider the case of no convection in the liquid. In a crucible of length L, shown in Figure 1, the first solid forming at the left end of the crucible has a composition given by kC_o. The solute that is rejected in the liquid is transported by diffusion only and an enriched "solute boundary layer" forms and gradually increases in solute. If the crystal is long, then a "steady state" is approached as shown in Figure 1b. At this "steady state", the composition of the solid forming is the overall composition C_o. Equilibrium at the interface requires that liquid composition at the interface be C_o/k and that solidification be occurring at T_s. Solute distribution

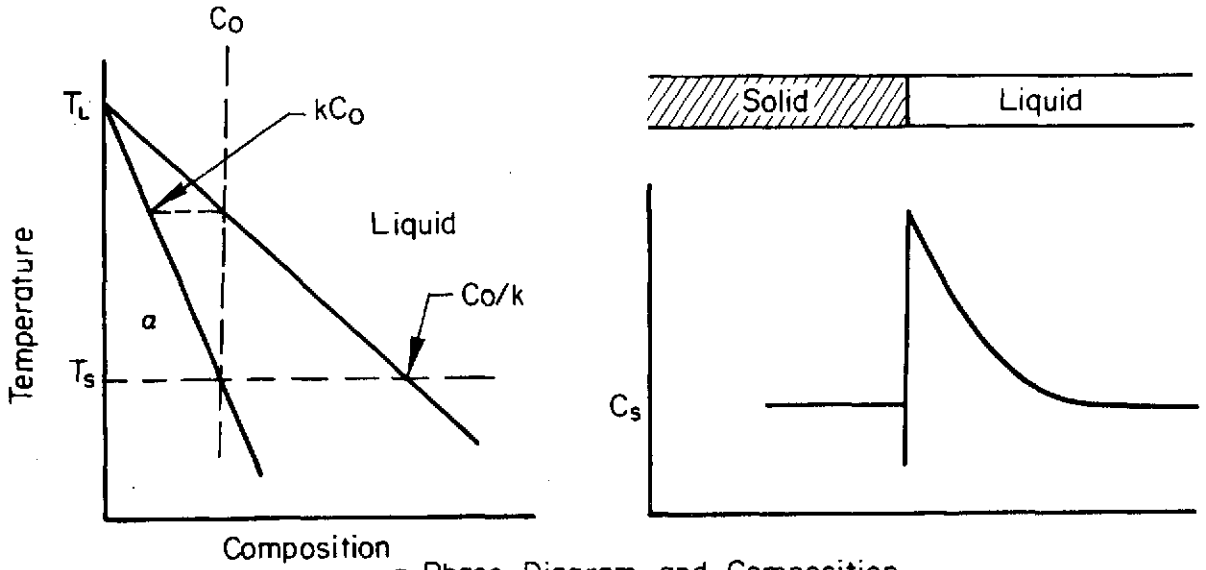

a. Phase Diagram and Composition Profile at "Steady State"

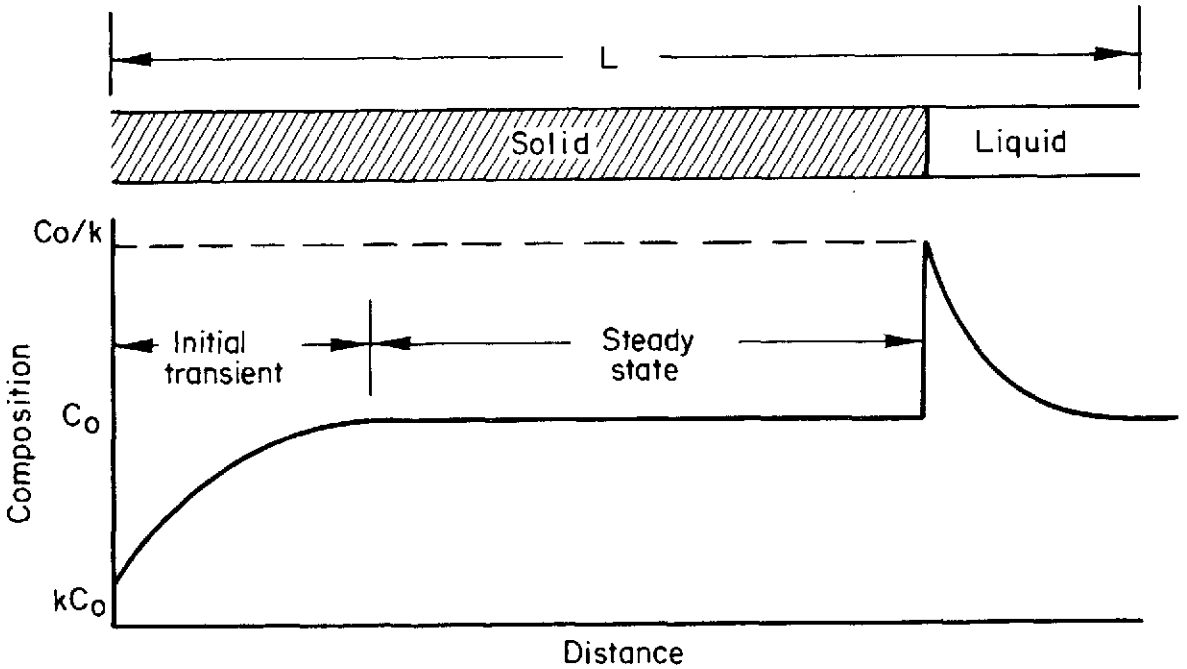

b. Composition Profile Showing Solute Distribution Along the Crystal

FIGURE 1. SOLUTE REDISTRIBUTION IN PLANE FRONT SOLIDIFICATION OF A SOLID SOLUTION WITH NO CONVECTION AND LIMITED LIQUID DIFFUSION

in the boundary layer in front of the interface has been solved by Tiller, Jackson, Rutter, and Chalmers[1] and is given by

$$C_L = C_o \left[1 + \frac{1-k}{k} \exp\left(1 - \frac{R}{D_L}\, x'\right)\right] \quad , \tag{3}$$

where

x' = distance from the liquid-solid interface

D_L = diffusion coefficient of solute in the liquid.

D_L/R is defined as a "characteristic distance" (i.e., distance at which the quantity $(C_L - C_o)$ falls to 1/e of the maximum $(C_o/k - C_o)$.

The solidification conditions described above result in a crystal of nearly uniform composition except for the initial transient, shown in Figure 1, and a final transient occurring at the other extremity. The initial transient forms while the solute boundary layer builds up to its maximum "steady state" value. Quantitative description of solute redistribution and the extent of the initial transient have been published by Smith, et al[4]. Their results indicate that the distance x required to reach "steady state" depends on R/D_L and k.

Of particular importance in this study is the effect of changes in interface velocity during solidification on the corresponding solute redistribution. Such changes occur due to convection. Figure 2 shows the effect on solute redistribution when the interface velocity is abruptly increased. Since a change in interface velocity also changes the characteristic distance, then the excess solute that was initially in the boundary layer (after interface velocity was increased) must now appear as a solute-rich "band" in the crystal. This is shown schematically in Figure 2.

Effect of Convection

For the case where convection in the liquid is present, solute redistribution is given by the Burton, Primm, and Slichter[5] equation. In this treatment, a diffusion boundary layer of thickness δ is assumed. Outside this layer complete mixing in the liquid by convection is assumed, and inside this layer mass transport is by diffusion only. Figure 3 shows the type of boundary layer discussed in this section. If

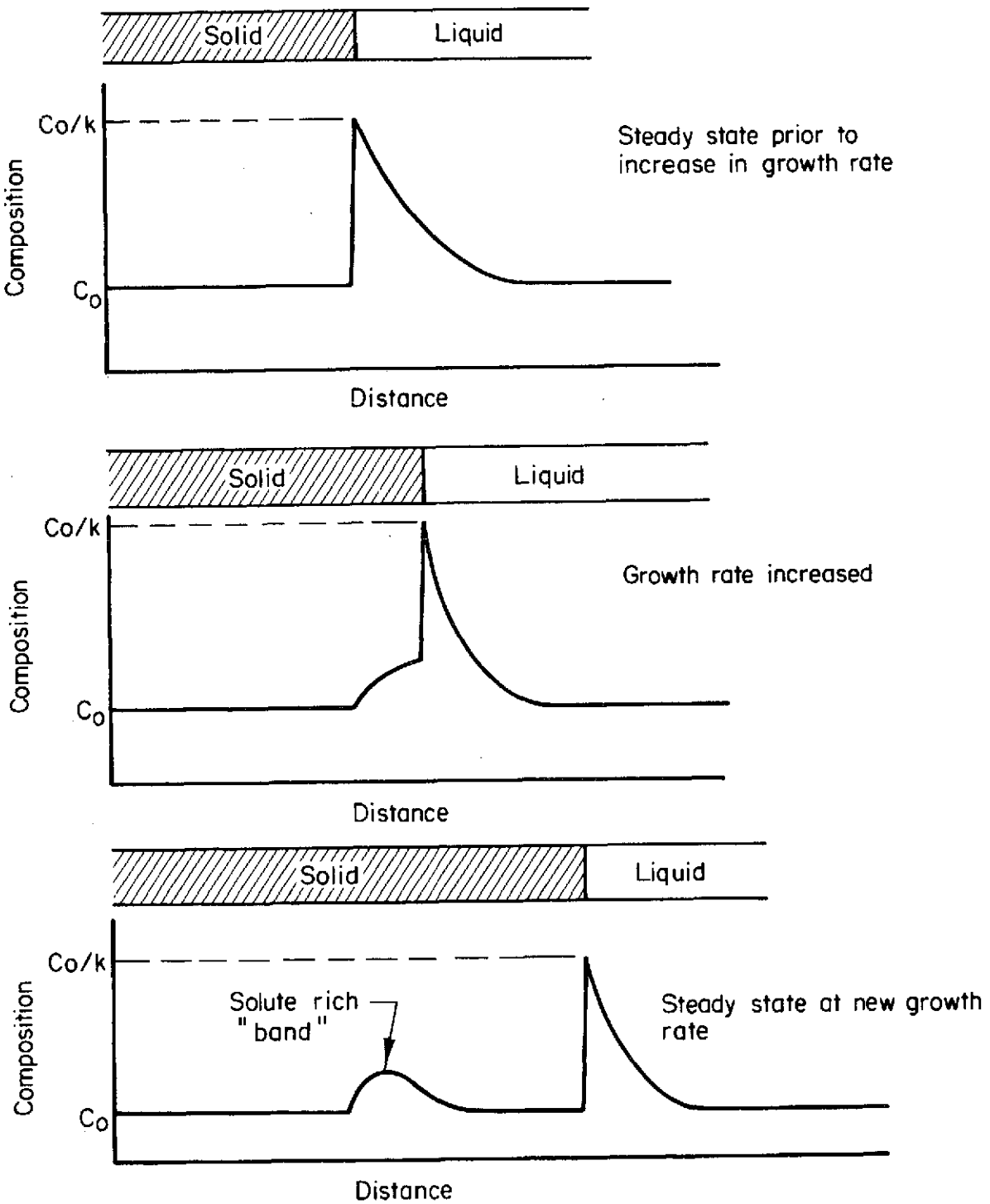

FIGURE 2. INCREASE IN GROWTH RATE (INTERFACE VELOCITY) RESULTING IN SOLUTE-RICH "BAND"

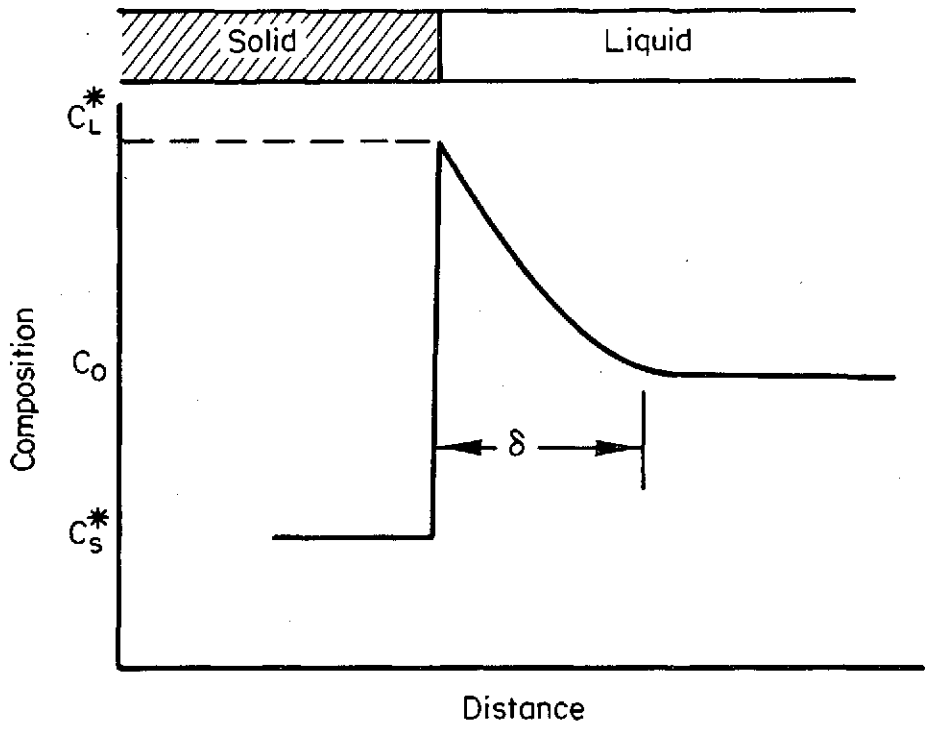

FIGURE 3. SOLUTE REDISTRIBUTION IN THE LIQUID IN THE PRESENCE OF CONVECTION

solidification is occurring in a very large liquid bath, then the bulk liquid composition remains essentially constant at C_o. A "steady state" solution to the problem yields the following equation:

$$\frac{C_L^* - C_s^*}{C_o - C_s^*} = \exp\left[\frac{R\delta}{D_L}\right] \quad . \tag{4}$$

An "effective partition ratio", k', is now defined as the ratio of the solid composition forming, C_s^*, to the bulk liquid composition (in this case, C_o). Then, substituting in Equation (4), we get

$$k' = \frac{k}{k + (1-k)\exp\left[-\frac{R\delta}{D_L}\right]} \quad . \tag{5}$$

This expression now relates composition of the solid forming to the initial alloy composition. Equation (5) can also be used to describe solute redistribution in finite (small) crucibles, provided that δ (boundary layer) is small compared to the length of the crucible. If this is true, then an equation identical to the Scheil equation can be written, except that the equilibrium partition ratio, k, is replaced by the effective partition ratio, k':

$$C_s^* = k' C_o (1-f_s)^{k'-1} \quad . \tag{6}$$

In this case the bulk liquid composition is C_L and $k' = C_s^*/C_L$.

In the limiting case when convection in the liquid is stopped (i.e., in the absence of gravity or by imposing a transverse magnetic field on the liquid), then a maximum value of k'-1 is obtained ($R\delta/D_L >> 1$). Under this condition, solute distribution is described by the special case of no convection given in the preceding section.

From the quantitative expressions presented here, it can be seen that changes in growth velocity, R, or solute boundary layer, δ, will have a corresponding effect on the solute distribution of the growing crystal. For example, increasing R and δ results in an increase in C_s^*. Fluctuations of R or δ during solidification of the crystal result in solute "banding" as previously described. It has been shown that these fluctuations are caused by temperature fluctuations that can be produced by furnace temperature instability and turbulent thermal convection in

the melt near the interface[6], and/or by a form of convection instability called "overstability"[7] when convection flow is in the laminar range.

Homogeneity in solid-solution alloy single crystals can only be obtained if growth rate (interface velocity) and convection (i.e., boundary layer, δ) are constant during solidification. Some causes of growth perturbations can be eliminated if they are external to the melt, such as power input, vibrations, etc. A much more difficult source to eliminate is that resulting from a density gradient in the liquid. As stated previously, these density differences result from differences in composition or temperature. Several studies have shown that density differences due to temperature gradients result in considerable flow in different crystal-growing techniques[8-11]. These types of convection patterns, which are turbulent, result in temperature fluctuations which in turn perturb the growth rate of the liquid-solid interface and cause "banding".

An important (dimensionless) parameter in thermal convection is the Rayleigh number[3]

$$R_a = \frac{L^3 \beta g \Delta T}{\alpha \nu} \quad , \tag{7}$$

where

L = the dimension (length of the container)

β = the volume coefficient of thermal expansion of the liquid metal

g = the gravity acceleration constant

ΔT = the temperature difference over length, L

α = the thermal diffusivity of the liquid

ν = the kinematic viscosity of the liquid.

For typical conditions of metal crystal growth, Rayleigh numbers are large (ca 10^5), and it is to be expected that convective flow is in the turbulent range. It should be noted that, although only one set of dimension and temperature-gradient vectors appear in the expression for R_a, it has been concluded[12] that thermal convection is dependent upon both longitudinal and transverse temperature gradients.

The majority of studies of thermal convection and its effects on crystallization in metal crystal-growth melts have been conducted with

horizontal growth systems (wherein the effects may be maximal). There is need to investigate the phenomena more comprehensively in the vertical growth regime.

Some temperature fluctuations can be avoided by improving on growth-furnace stability and temperature control. Constitutional supercooling can be avoided by reducing the growth rate and/or maintaining a steep temperature gradient across the solid-liquid interface. The latter, however, will tend to increase convective flow and the resulting thermal fluctuations. It is apparent at this point in the discussion that, while the just mentioned gross temperature fluctuations that produce coarse banding and constitutional supercooling can be eliminated by modifying growth conditions in straightforward and attainable ways; thermal convection and the temperature fluctuations produced thereby cannot be eliminated by such straightforward means when the growth system is on earth and in its gravity field. Thus, there is justification for investigation of "zero-gravity" crystal growth and the effects on substructure of the crystals.

Although the gravity field cannot presently be eliminated in terrestrial laboratories, it has been found that a magnetic field can be used to counteract its effects with respect to convection. The convection in liquid metallic systems can be impeded by imposing a steady magnetic field on the liquid. Utech and Flemings[11] have shown that a magnetic field can be used to damp liquid convection, suppress the fluctuations, and in turn eliminate solute-rich "bands".

Flow of a conductive liquid across a magnetic field is strongly damped as a result of inductive drag. This drag can be regarded as a magnetic "viscosity". According to Chandrasekhar[13], application of the field imparts an effective kinematic viscosity to the liquid. The value of this "viscosity" is given by

$$v_{eff} = \mu^2 H^2 \sigma d^2 / \rho \quad , \tag{8}$$

where

μ = magnetic permeability of the liquid

H = strength of the magnetic field

σ = electrical conductivity of the liquid

d = depth of the liquid

ρ = density of the liquid.

The magnetic viscosity can be significant and dominant if the Hartmann number, M, is large compared with unity[14]. M is defined as

$$M^2 = \frac{\sigma(\mu HL)^2}{\rho\nu} = \frac{\text{magnetic viscous forces per unit volume}}{\text{ordinary viscous forces per unit volume}} \quad , \quad (9)$$

where

μ = the magnetic permeability

H = magnetic field strength

σ = the electrical conductivity

L = the length of the melt

ρ = the density

ν = the kinematic viscosity of the liquid metal.

For typical metal systems, estimates made from this expression indicate that only modest magnetic fields, on the order of 10^3 gauss, are required to effectively damp out turbulent temperature fluctuations and eliminate "banding".

In a recent study[15] of magnetic field effects on dense liquids, Henderson and Miller examined several models to characterize liquid behavior. The Free Volume Model originally developed by Turnbull[16] and Cohen[17-19] appeared to best represent the liquid state in a magnetic field. Henderson and Miller[15] showed that the application of a magnetic field or removal of the gravitational field would result in an increase in liquid volume and free energy and a subsequent increase in the diffusion coefficient of the solute species, leading to higher crystal growth rates.

Thus, the use of a magnetic field applied during the crystal growth of metal solid solution alloy appears to offer an excellent means of simulating "zero-gravity" growth and of assessing expected effects on the substructure and homogeneity of solid-solution material so prepared.

Growth Conditions for the Selected Alloy System

It was recognized as desirable that the binary solid-solution alloy chosen for study should, as a minimum, have a range of solid solution,

melt in the appropriate temperature range, have a reasonable liquidus-solidus separation, and be readily obtainable in high purity. Silver and zinc are readily available in high purity and, as can be seen from the phase diagram (Figure 4), the alpha phase region of the silver-zinc system meets the other three of these basic requirements. Other factors such as the slope of the liquidus, solid-state diffusion rate, density-temperature, and density-composition relations were recognized as being important with respect to segregation and the generation of convection currents.

As a first step in the experimental program, available properties of the selected silver-zinc system were used to calculate the growth conditions required.

Temperature Gradient and Growth Rate

It is recalled that the criterion for a stable plane interface is given by

$$\frac{G}{R} \geq -\frac{mC_s(1-k)}{kD_L} \approx \frac{m(C_s-C_L)}{D_L} \quad , \tag{10}$$

where

G = temperature gradient in liquid

R = rate of growth

m = slope of liquidus

C_s = composition of solid at interface

C_L = composition of liquid at interface

k = segregation coefficient, C_s/C_L

D_L = diffusion coefficient of solute in the liquid.

From the phase diagram and literature on diffusion, the pertinent properties of αAg-20Zn at 800 C were estimated to be the following:

Slope of liquidus, $m = 7$ C/at. %

Composition of solid at interface, $C_s = 17$ at. % Zn

Composition of liquid at interface, $C_L = 22.5$ at. %

Diffusion coefficent of solute in melt (estimated),

$D_L \sim 2 \times 10^{-4}$ cm^2/sec.

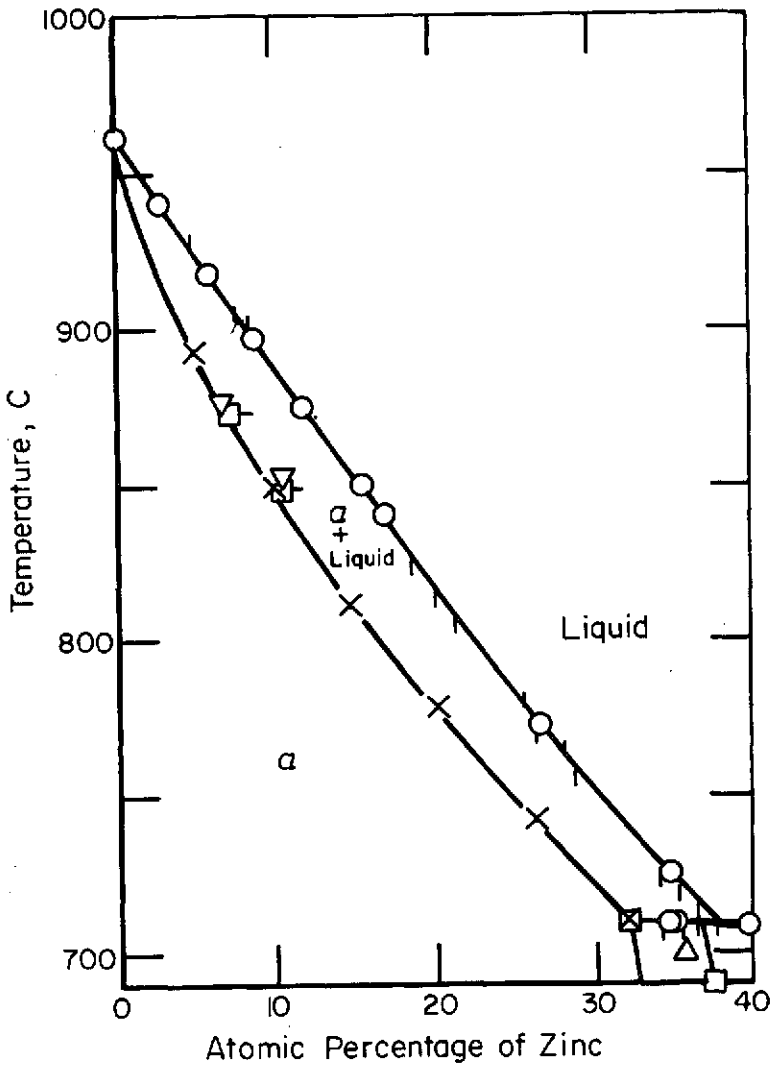

FIGURE 4. PORTION OF THE SILVER-ZINC EQUILIBRIUM DIAGRAM[20]

Utilizing these values, the critical condition for a stable, plane interface for Ag-20Zn at the liquidus temperature (∿ 820 C) is

$$\frac{G}{R} > \frac{7 \times 5.5}{2 \times 10^{-4}} \simeq 2 \times 10^{5} \frac{C \text{ sec}}{cm^2} \quad . \tag{11}$$

From this, several sets of potentially useful temperature gradient-growth rate conditions for planar-interface growth are seen to be as follows.

For G =	R should be <
10 C/cm	5×10^{-5} cm/sec = 1.8 mm/hr
25 C/cm	12.5×10^{-5} cm/sec = 4.5 mm/hr
50 C/cm	2.5×10^{-4} cm/sec = 9 mm/hr

Crucible Size

It is recalled that the Rayleigh number which gives the basis for selection of container size is given by

$$R_a = \frac{L^3 \beta g \Delta T}{\alpha \nu} \quad , \tag{12}$$

where

L = characteristic length of container
β = volume coefficient of thermal expansion of the liquid metal
g = gravity acceleration constant
ΔT = temperature difference over length L
α = thermal diffusivity of the liquid
ν = kinematic viscosity of the liquid.

Using the best available or best estimated values for αAg-20Zn, the Rayleigh number is estimated to be

$$R_a = \frac{L^3 \times 6 \times 10^{-5} \times 980 \, \Delta T}{4 \times 10^{-3}} \quad . \tag{13}$$

Choosing several sets of potentially useful values for crucible length and temperature gradient, estimates of Rayleigh number for the indicated conditions are as follows:

For L = 2 cm, $L^3 = 8$, then $R_a \simeq 120\ \Delta T$, and for

$\Delta T = 10$ C, $R_a = 1.2 \times 10^3$

$\Delta T = 20$ C, $R_a = 2.4 \times 10^3$

$\Delta T = 50$ C, $R_a = 6 \times 10^3$

$\Delta T = 100$ C, $R_a = 12 \times 10^3$.

For L = 5 cm, $L^3 = 125\ cm^3$, then $R_a \simeq 1.9 \times 10^3 \times \Delta T$, and for

$\Delta T = 25$ C, $R_a = 4.8 \times 10^4$

$\Delta T = 50$ C, $R_a = 9.5 \times 10^4$

$\Delta T = 125$ C, $R_a = 2.4 \times 10^5$

$\Delta T = 250$ C, $R_a = 4.8 \times 10^5$.

Since $R_a \geq \sim 10^3$ permits turbulent flow, it can be seen that any L > 2 cm is satisfactory for use in this investigation. The minimum dimensions of crucibles utilized in this study were length = 11 cm, width = 1.5 cm, height = 1 cm.

Magnetic Field Strength

As has been discussed previously, the magnetic viscosity can be significant and dominant if the Hartmann number, M, is large compared with unity. M is defined as

$$M^2 = \frac{\sigma(\mu HL)^2}{\rho\nu} = \frac{\text{magnetic viscous forces per unit volume}}{\text{ordinary viscous forces per unit volume}} , \quad (14)$$

where

μ = magnetic permeability

H = magnetic field strength

L = characteristic length of melt

ρ = density

ν = kinematic viscosity

σ = electrical conductivity.

For $\rho\nu \approx 3.4 \times 10^{-2}$ poise (g/cm sec), $\sigma = 5 \times 10^{-5}$ abohm^{-1}cm^{-1}, H (oesteds) = B/μ, and $\mu = 1$,

$$M^2 = \frac{5 \times 10^{-5}}{3.4 \times 10^{-2}} (\mu HL)^2 \approx 1.5 \times 10^{-3} (BL)^2 \quad . \qquad (15)$$

Since L is the characteristic length for current flow--i.e., fluid (conductor) flow from hot to cold regions--and is of the order of 2-5 cm minimum in the experimental apparatus, evaluation of the Hartmann number for several potentially useful sets of conditions can be made:

	B, gauss					
	200		500		1000	
L, cm	M^2	M	M^2	M	M^2	M
2	240	15	1500	39	6000	78
5	1500	39	9370	97	37,500	194
10	6000	78	37,500	194	1.5×10^5	387

From this it can be seen that $M >> 1$ and magnetic viscosity is dominant for magnetic fields equal to, or greater than, several hundred gauss.

Crystal-Growth Apparatus

The crystal-growth apparatus for producing the required growth conditions, along with ancillary equipment for making the observations desired, was designed and built. The experimental apparatus consists of four major components, which are shown from left to right in Figure 5:

(1) The stabilized magnet power supply
(2) The two stepless saturable-core-reactor controls for the crystal-growth furnace
(3) The 4-in. electromagnet unit with the specially designed and built crystal-growth furnace in place between the pole and pieces
(4) A fast-response recording potentiometer.

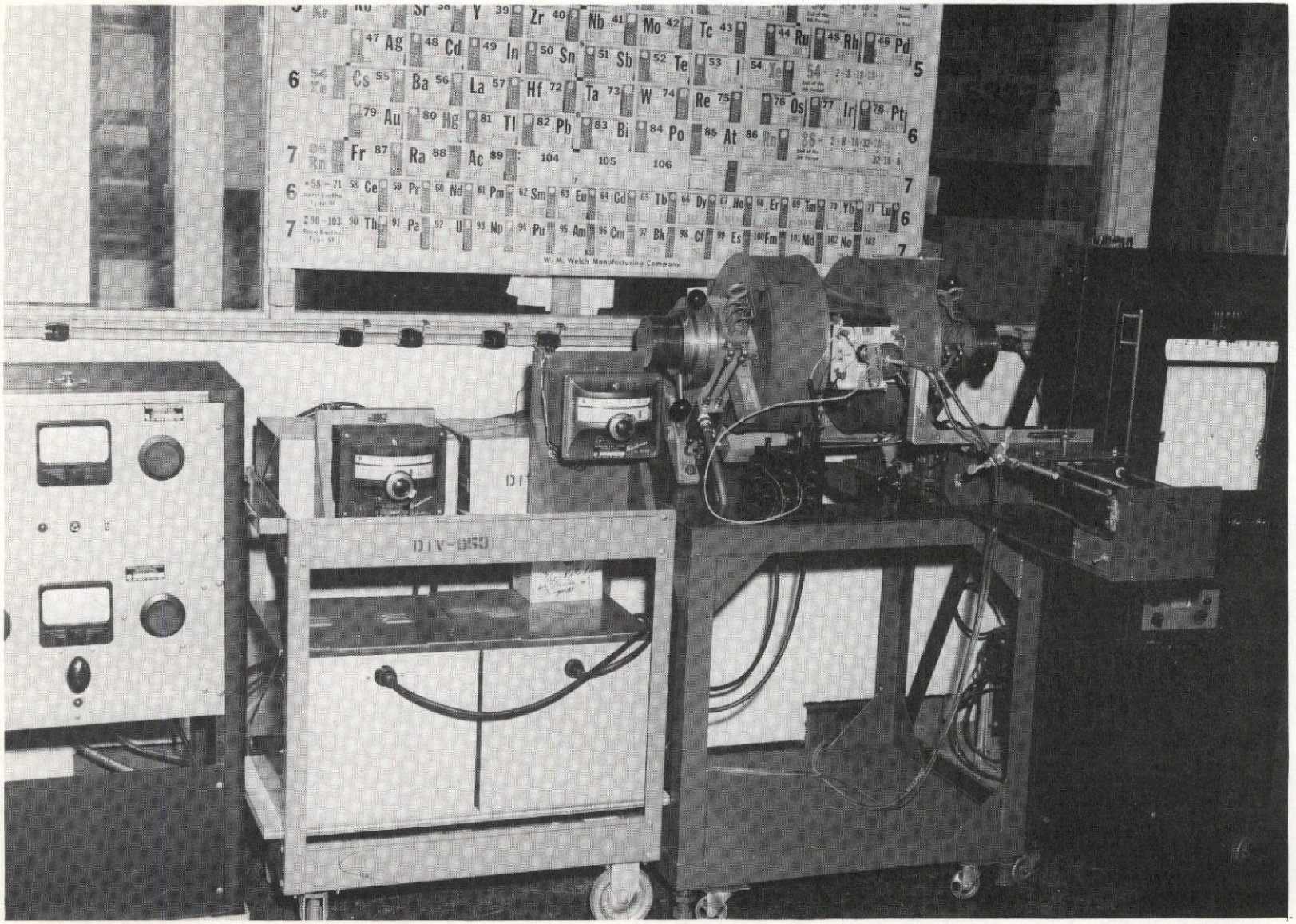

FIGURE 5. CRYSTAL-GROWTH APPARATUS

The magnet unit and crystal-growth furnace are shown set up for horizontal crystal growth. However, the apparatus is designed for rapid conversion to vertical growth and growth at other angles to the gravity vector.

The growth tube is shown in place with the thermocouple leads attached to the thermocouple switching unit. Provision was made for the use of up to five thermocouples accurately placed in the alloy charge. The screw drive that is used to move the crystal-growth crucible can be seen at the right front of the magnet unit; it is driven by a synchronous motor and the movement rate is controlled by gears in the drive train.

The bearing surfaces for movement of the crystal-growth tube are of the sliding type and are contained within and are integral parts of the furnace (see Figure 6). The outer bearing is made of graphite, while the centrally located bearing is a disc of boron nitride, which also serves as a baffle between the two independently controlled furnace heating segments. The furnace readily attains 1000 C chamber temperatures with negligible heat flux to the magnet poles. The seal and feedthroughs at the exposed end of the crystal-growth tube are water cooled, and a water-cooled copper chill is provided for the cooling of the heat sink and low-temperature end of the growth crucible as required.

General Procedures and Information

Macroscopically, homogeneous supplies of the Ag-20Zn alloy were prepared from 99.999 percent purity metals by melting, homogenizing, and chill casting in an inert argon atmosphere. The alloy was cleaned prior to loading into the growth crucible by use of an etch solution containing 7.6 g/l of CrO_3 and 8 g/l of H_2SO_4. After the material was loaded into the growth tube, the tube was evacuated and flushed several times with pure helium, then was sealed with approximately 2/3 atmosphere of helium.

The required crystal-growth crucibles were machined from high-purity graphite and were outgassed prior to use at 1000 C in vacuum.

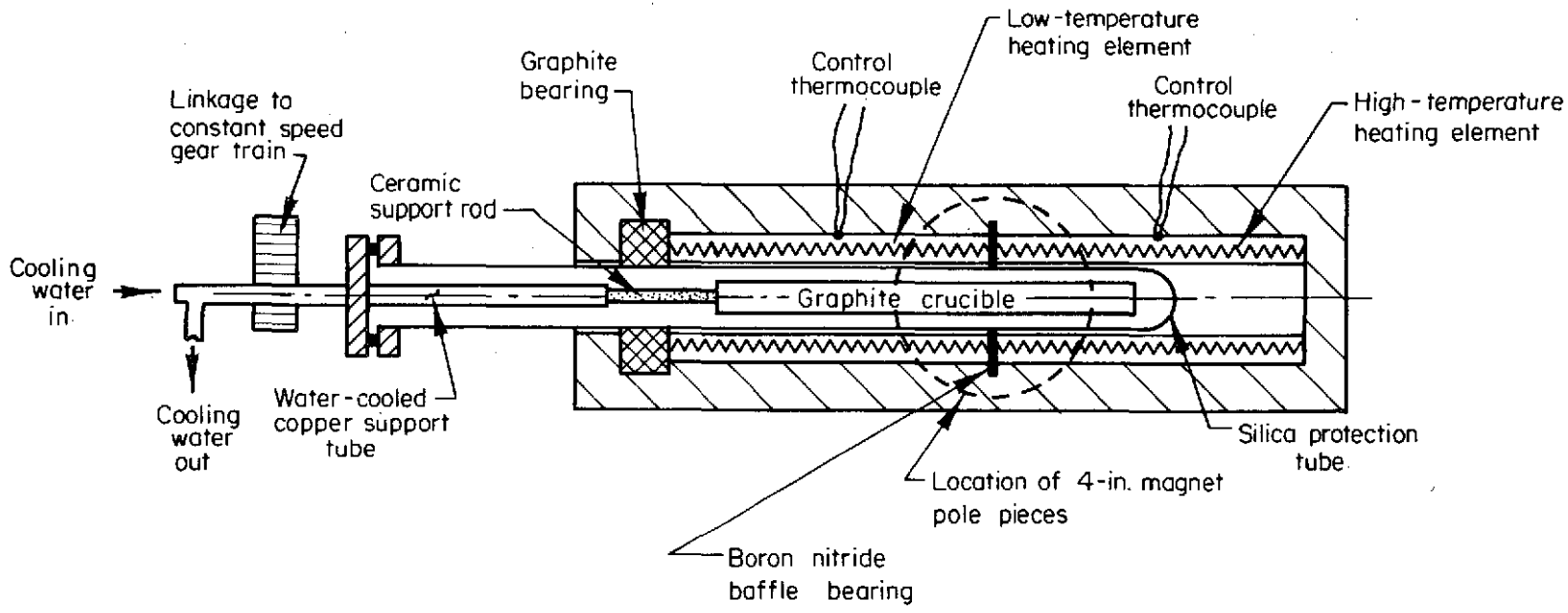

FIGURE 6. SCHEMATIC OF CRYSTAL-GROWTH FURNACE

Graphite appeared to be entirely satisfactory as a crucible material, as there was no apparent chemical interaction between the melt and the graphite. With the 2-mm wall thickness that was employed, results of initial exploratory runs indicated that the thermal conductance of the graphite would not interfere with the desired processes: the solid/liquid interfaces in the alloy were observed to be planar (on a gross scale with the system at rest), and temperature gradients in the desired range were established without difficulty.

Fine-gauge thermocouples that were used to monitor temperatures in the melt were chromel-alumel sheathed with Type 304 stainless steel. Both 0.010-in.-OD and 0.020-in.-OD thermocouples were used; no significant difference between sensitivities of the two sizes was observed. Even after prolonged periods at elevated temperatures, there was no detectable attack of the molten Ag-Zn alloy on the stainless steel thermocouple sheath. However, in about the 400-C zone, zinc condensed on the thermocouples and diffused into the sheath material, causing embrittlement and failure after several runs.

Although there was some loss of zinc from the melt by vapor transport, this appeared to occur primarily at the time the charge was initially melted, and the rate of transport appeared to decrease to a negligible level thereafter. The results of postgrowth analyses indicated that shifts in composition were not significant. However, floating covers of $\sim$ 2-mm-thick graphite were used to further reduce the rate of loss of zinc from the melts.

Investigation of Convection

A study was made of the characteristics and effects of convection currents in the molten Ag-20Zn alloy in a horizontal boat. The temperature fluctuations resulting from the convection currents were monitored while overall longitudinal temperature gradients of 1.5, 2.5, 5.5, 7.5, 8, 12, and 16.5 C/cm were imposed on the melt.

No significant short-term temperature fluctuations (i.e., periods < 30 seconds) were observed with longitudinal temperature gradients < 8 C/cm. With these low-temperature gradients, short-term fluctuations were $\lesssim$ 0.005 mv ($\approx$ 0.1 C) and may have resulted from "noise" of the system. Some long-term fluctuations were observed with periods of 10 to 20 minutes and maximum peak-to-peak amplitudes of 0.01 mv ($\sim$ 0.24 C); however, in view of the low magnitude, these did not appear to be significant.

With overall longitudinal temperature gradients of 12 and 16.5 C/cm imposed on the melt, significant short-term temperature fluctuations such as are shown in Figures 7a and 8a were observed. Typically, these appeared to be a combination of two or more oscillations having different frequencies, with the result that amplitude peaks varied in magnitude as the oscillations reinforced or opposed one another. Maximum amplitudes (peak-to-peak) observed were in the range of 0.02 to 0.06 mv ($\sim$ 0.5 to 1.4 C), and periods of the short-term oscillations were observed to be in the range of 6 to 10 sec.

No direct relationship between the magnitude of the temperature gradient and the amplitude or period of the temperature oscillations was apparent.

Investigation of the Effects of Magnetic Field

The effect of a magnetic field on convection currents in the molten Ag-Zn alloy, as revealed by the effect on temperature oscillations in the melt, was investigated. Magnetic fields in the range from 50 to 4000 gauss were applied to the melt under the various sets of conditions discussed in the previous section, and the effect on the temperature oscillations was recorded. As can be seen in examples of results presented in Figures 7a-e and 8a-d, moderate magnetic fields (e.g., 50 to 250 gauss) decrease the overall amplitude and damp out some of the multiple oscillations, in most cases reducing the oscillations to a single frequency of moderate amplitude (Figures 7c and 8c). At a sufficiently high field strength, the short-term temperature oscillations that are attributed to turbulent convection are damped out (Figures 7d and 8d). The field

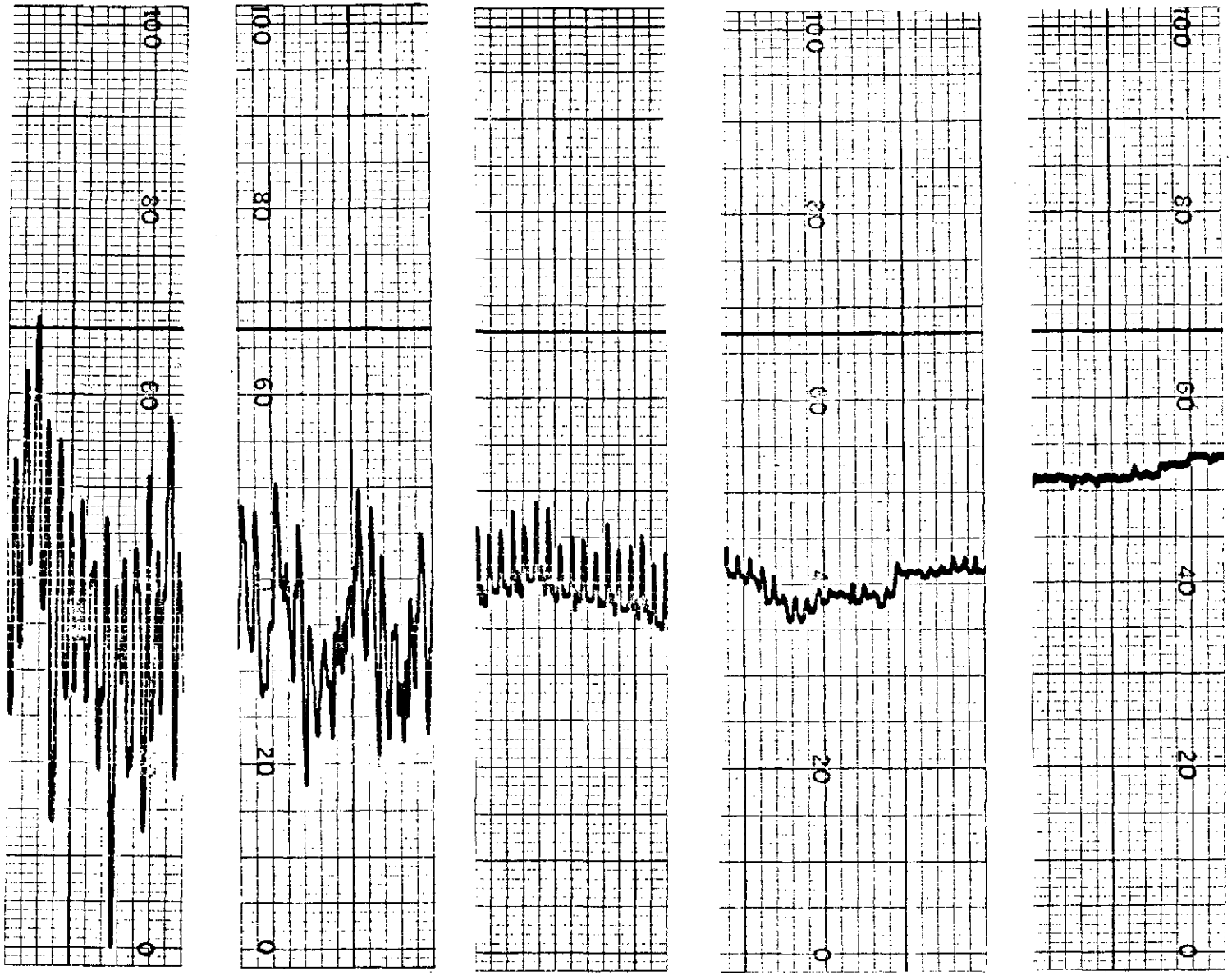

(a) No magnetic field (b) 200 gauss (c) 300 gauss (d) 350 gauss (e) 500 gauss

FIGURE 7. TEMPERATURE FLUCTUATIONS IN Ag-20Zn MELT IN HORIZONTAL BOAT

857 C; G = 13 C/cm; chart speed 2 min/in.:
0.1 mv ≈ 2.44 C full scale.

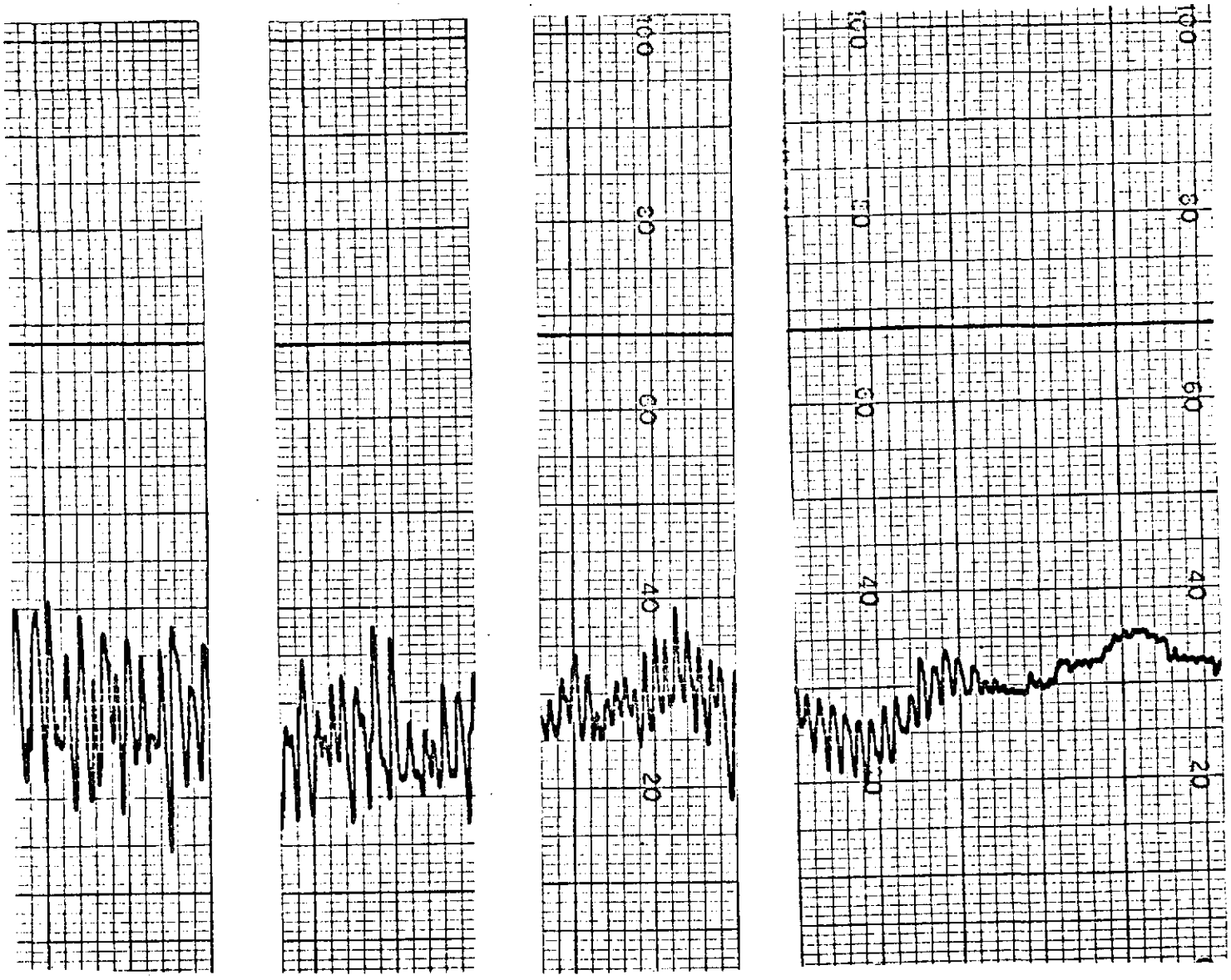

(a) No magnetic field (b) 100 gauss (c) 200 gauss (d) 300 gauss

FIGURE 8. TEMPERATURE FLUCTUATIONS IN Ag-20Zn IN HORIZONTAL BOAT

869 C; G = 13/cm; chart speed 2 min/in.;
0.1 mv ≈ 2.44 C full scale.

strengths required to do this were found to be 300 to 350 gauss--in good agreement with values anticipated for the Ag-Zn alloy as a result of the Hartmann-number analysis. Magnetic fields of higher strengths (1000, 1500, 2000, 3000, and 4000 gauss) were found to have no detectable effect on the convection-current-related temperature oscillations beyond that observed with the 350 to 500-gauss fields.

Crystal Growth

Crystallization runs were made to (1) check out the apparatus under crystal-growth conditions and (2) produce samples containing "typical" microstructural features that could be used in the development of characterization techniques. The crystallizations were run under conditions expected to produce constitutional supercooling ($G/R < 2 \times 10^5$ C sec/cm^2 at 800 C), with a temperature gradient of $\sim$ 25 C/cm and linear movement rates of 0.62 and 1.5 cm/hr. In addition, portions of the ingots were air quenched at the conclusion of the run to obtain dendritic growth material for examination.

Several vertical Bridgman crystal growth cycles were made, primarily to obtain monocrystalline seed material to be used in the controlled crystal-growth experiments. This material also was examined metallographically as part of the longitudinal sections of some of the seeded alloy ingots. For the vertical Bridgman crystal growth, the material was contained in a cylindrical graphite crucible which was sealed in a silica protection tube under a pressure of about 2/3 atmosphere of pure helium. The crystals were grown at a rate of 0.9 mm per hour using either rf induction or electrical resistance heating.

When seeding was used, the seed crystal was cut to fit the crucible. The work-damaged layers were removed by etching, and the seed crystal was pinned in place at the head of the charge by use of graphite pins. Monitoring of the position of the intersection of the temperature gradient with the liquidus temperature was used to obtain controlled melting of the seed crystal.

A number of crystallization runs were made in the horizontal mode under conditions calculated to produce constitutional supercooling

and under conditions calculated to give planar-interface growth; these early runs were not seeded. Using single-crystal seeding, horizontal growth runs were also made under similar conditions; in these runs, sections were grown with and without applied transverse magnetic fields of several strengths (500, 1500, and 4000 gauss). Data on representative controlled-growth runs are given in Tables 1 and 2.

Because of the limited length of the crucible and the limitations in the heat sink, the position of the solid-liquid interface is displaced as the major portion of the alloy charge is moved from the high-temperature to the low-temperature furnace segment. Thus, the effective interface movement rate is higher than the drive unit movement rate; at the low travel rate of 1 mm per hour, the effective interface movement rate is approximately 2 mm per hour. Where noted in Tables 1 and 2, the effective rate has been used to obtain G/R ratios.

Ingots 31012-16, -19, and -21 (Table 1) were grown with alternate sections subjected to a 500-gauss magnetic field. No magnetic field was applied during growth of the intervening sections.

In a planned matrix of experiments, growth was investigated in four zones as indicated in Table 2. Controlled growth in three zones at a constant movement (growth) rate in the planar-interface growth mode was conducted with high, moderate, and no magnetic field applied. Since in the early runs it was found that the 400-gauss field produced no observable effect on cellular growth, 1500 gauss was substituted as the moderate field strength in the later experiments. In the initial zone, seeding and initial crystal growth were observed. In the intermediate zones, crystal growth and growth orientation were studied. In the final cool-down zone, cellular and dendritic growth at various rates (with and without applied magnetic fields) were investigated. Metallography was used in all regions to detect differences in microstructure.

It should be noted (Tables 1 and 2) that while G/R values for the cellular growth experiments are nearly an order of magnitude smaller than the estimated boundary G/R value (2×10^5 C sec/cm^2), those for the planar-interface (banding) growth experiments are only 2 to 3 times greater than the boundary value. This could possibly explain why cellular growth

TABLE 1. DATA ON EXPLORATORY CRYSTAL GROWTH EXPERIMENTS

Experiment	Growth Desired	R,[a] mm/hr	G, C/cm	G/R, C sec/cm^2	H, gauss
31012-7	Cellular	15	15-28	$3.5 - 6.5 \times 10^4$	0
31012-11	Banded	1.8(3.6)	8-35	$0.8 - 3.5 \times 10^5$[b]	0
31012-13	Banded	1(2)	7-38	$1.2 - 6.8 \times 10^5$[b]	0
31012-16	Banded	1(2)	9-14	$1.6 - 2.5 \times 10^5$[b]	0, 500
31012-19	Cellular	15	13-18	$3.2 - 4.2 \times 10^4$	0, 500
31012-21	Banded	1(2)	14-19	$2.5 - 3.5 \times 10^5$[b]	0, 500

(a) R effective is listed in parentheses.

(b) Calculated using R effective.

TABLE 2. DATA ON CRYSTAL GROWTH EXPERIMENTS

Experiment[a]	H, gauss			Terminal Growth (Cool-down) Zone		G, C/cm	G/R, C sec/cm^2
	Seeding and Initial Growth	Growth Zone II	Growth Zone III	H, gauss	Cooling Rate, C/min		
31012-23	0	400	400	4000	11	13 to 23	2 to 4 x 10^5
31012-27	4000	0	1500	0	13	17 to 19	3 to 3.4 x 10^5
31012-29	0	1500	4000	1500	7	16 to 20	2.9 to 3.6 x 10^5
31012-31	1500	4000	0	4000	22	14 to 20	2.5 to 3.6 x 10^5
31012-34	0	4000	0	500	7	23[b]	4.1 x 10^5

(a) For all experiments, growth was horizontal and a movement rate of 1 mm/hr was used; this gave an effective interface movement rate of approximately 2 mm/hr.

(b) Thermocouples failed and values were obtained through only the first portion of the run.

has been observed while banding has not. Accordingly, for the last two runs, the growth system was modified with the objective of increasing the temperature gradient, G, thus creating growth conditions more strongly favoring banding. For Run 31, the size of the low-temperature heat sink was increased and temperatures of the two furnace zones were set farther apart. For Run 34, the lengths of the crucible and ingot were increased, thus further increasing the size and effectiveness of the heat sinks. In spite of these modifications, the G values were no larger than the maximum values obtained previously through portions of growth runs (See Table 1). Since the measures taken have gone to the practical limits of the present apparatus, it appears that the conditions required to obtain higher G/R values are not obtainable without major modification of the growth system. (Reducing the cross-sectional area of the ingot is not feasible since a minimal cross-sectional dimension must be maintained or convectional flux will be eliminated.) In addition, because of the high melting point and high thermal conductivity of the Ag-Zn alloy (relative to those of low-melting-temperature metals and semimetallic or semiconductor systems with which this type of investigation has been conducted previously by others), it will be more difficult to achieve and sustain higher temperature gradients (and G/R ratios) with this system while still maintaining the stability required for crystal growth.

Characterization and Analysis

Utilizing material from the initially available polycrystalline ingots, required metallographic techniques applicable to the Ag-Zn alloy were developed. The general procedure as developed for the preparation of Ag-Zn alloy sections for metallographic examination is as follows:

(1) Manual lapping on SiC paper through 600 grit
(2) Manual lapping on No. 600 soft alumina paper
(3) Finish polishing with 1-μ diamond on lintless jersey on a vibratory polisher

(4) Chemical polishing (by swabbing) for about 30 sec with a reagent containing 7.6 g/ℓ of CrO_3 and 8 g/ℓ of H_2SO_4

(5) Etching in the same reagent diluted 10:1.

Examination of ingots crystallized under conditions calculated to give constitutional supercooling has revealed the expected cellular growth. The results of electron microprobe analyses of the cellular structure indicate that cell-wall thickness and composition differ from ingot to ingot, presumably due to differences in crystallization rate and melt composition. An example of the cellular growth from Ingot 31012-13 is shown in Figure 9. This ingot was grown at 1 mm per hour. However, this cellular growth region ∿ 1 cm long was formed during the rapid freezing that occurred as the ingot was air quenched at the end of the run; beyond this, the growth became dendritic. The composition and size of cells were essentially uniform over the cellular section. This is consistent with its having been formed by rapid freezing and, therefore, being unaffected by diffusion in the solid after freezing. The results of electron microprobe analysis (Table 3) indicate that the cell walls were enriched in zinc by about 8 atomic percent above the matrix concentration of 21 atomic percent, and cell wall thicknesses were in the range from 60 to 120 μ.

Although compositional and structural features of the cellular growth have been essentially uniform within each specimen analyzed to date, relatively large variation from ingot to ingot has been observed, with cell-wall zinc enrichment (over matrix concentration) ranging from 3 to 9 atomic percent and apparent cell-wall thickness varying in the range from 25 to 120 μ.

There are indications that the cellular structure has been modified due to annealing of the solidified material in the growth furnace during the growth process. For example, examination of Ingot 31012-19, which was grown under conditions calculated to yield constitutional supercooling, revealed cellular growth over a considerable portion of the ingot. The cell walls appeared more diffuse in the portion of the metal held the longer time in the solid at elevated temperature. This has not been confirmed by electron microprobe analysis, however.

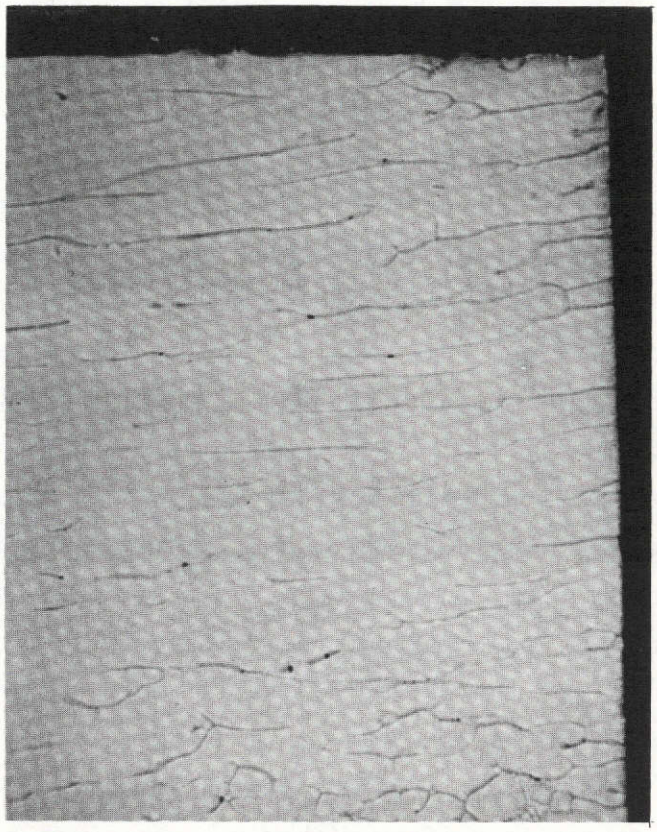

20X

31012-13

FIGURE 9. LONGITUDINAL SECTION SHOWING CELLULAR STRUCTURE IN Ag-20Zn INGOT DUE TO CONSTITUTIONAL SUPERCOOLING ($G/R < 2 \times 10^5$ C SEC/CM^2)

Crystallization direction: left to right.

TABLE 3. RESULTS OF ELECTRON PROBE ANALYSIS OF CELLULAR GROWTH IN INGOT 31012-13

Distance from Section End, mm	Zinc Concentration, at. %			Width, μ	
	Base	Peak	Δ	Base	1/2
1.8	21.1	29.4	8.3	94	52
2.8	21.1	30.4	9.3	100	62
3.8	21.8	27.9	6.1	58	32
4.8	21.9	28.4	6.5	60	36
5.8	21.3	29.5	8.2	89	56
6.6	21.4	29.7	8.3	126	78
7.8	21.4	28.3	6.9	108	60
9.1[(a)]	21.5	--	--	--	--

(a) The profile at 9.1 mm was taken at a point just beyond the last discernible cell wall.

Metallographic examination of some ingots grown under conditions calculated to give planar-interface growth, both with and without magnetic fields up to 4000 gauss, have revealed no obvious microstructural features.* Banding was not observed in any of the crystal-growth experiments, presumably because of the small spacing expected between the bands and the slow crystal-growth rates required for planar growth. The expected band spacing can be calculated from the average period, τ, of the turbulent convection currents (8 sec) and the growth rate (0.2 cm/hr) as follows:

$$\ell = \tau R = 4.4\ \mu \quad .$$

This interband spacing is extremely small and allows the bands to be eliminated by solid-state diffusion. This has been confirmed by using an analysis previously applied to a similar problem[3]. The largest half-band spacing, $\lambda = \ell/2$, which is eliminated by diffusion is given by

$$\lambda = \sqrt{D_s t} \quad , \tag{16}$$

where D_s is the effective interdiffusion coefficient in the solid and t the time held at this temperature. In the steady state, the solidified crystal is within 25 C of the solidus temperature (780 C) for 5 hours. The interdiffusion coefficient at this temperature is $\sim 2 \times 10^{-8}$ cm^2/sec. Thus,

$$\lambda = \sqrt{2 \times 10^{-8}\ (1.8) \times 10^{4}} = 190\ \mu \quad . \tag{17}$$

Accordingly, bands spaced < 380 μ apart should be eliminated by diffusion in the solid state.

In contrast with the microstructural observations, distinct changes in macrostructure were found to correlate with the application and removal of the magnetic field. For example, Ingot 31012-16, which was grown under conditions calculated to give planar-interface growth ($G/R \sim 5 \times 10^{-5}$ C sec/cm^2) both without and with a 500-gauss magnetic field, showed polycrystalline

---

* Only metallography has been applied thus far to the microstructural examination. Application of other techniques which are more sensitive to the defect structure, such as X-ray topography and transmission electron microscopy, is recommended.

growth (several large crystals) in the absence of the magnetic field and monocrystal growth in regions corresponding to the application of the magnetic field (Figure 10). Additional examples of the effect of magnetic field on crystal growth were noted (in Ingots 23, 27, and 31), wherein the number of crystals changed abruptly with the application or removal of the transverse magnetic field. The results of Laue X-ray diffraction analysis carried out on Ingot 31012-16 indicate that there is a preferred crystal growth direction within 5-7 degrees of the <100> direction independent of magnetic field (Figure 11). The single-crystal portions examined (Crystals 2 and 3 of Figure 11), which were grown during the application of a 500-gauss field, have approximately the same crystal orientation with respect to the growth direction and the longitudinal section examined. Although Crystal 1 (grown in the absence of a magnetic field) has a growth direction close to <100>, there is an orientation change relative to Crystals 2 and 3. The change can be described as a rotation of approximately 45 degrees around the growth axis. More study is required to determine whether the effect is a general one or related only to the crystals examined thus far.

An additional effect of magnetic field was noted in one ingot (23), where it was observed that crystal boundaries formed in a 4000-gauss magnetic field were curved and undulating, whereas boundaries grown without the magnetic field were planar. This effect of the magnetic field on crystal growth, per se, should be investigated further.

The fast-frozen portions of the first four ingots listed in Table 2 were observed to be of highly dendritic structure, as expected for a fast-frozen alloy of this type. Study of variations in the dendritic growth of the terminal rapid-growth region has revealed that there is an effect of magnetic field. As can be seen in Figure 12, the dendrites in Ingot 23, grown with a 4000-gauss field applied, appear finer and more highly oriented in the growth direction than those in Ingot 27, which were grown at the same rate (as deduced from the cooling rate) in the absence of a magnetic field. Extension of this effect also is seen in Ingot 29, where application of a moderate magnetic field appears to

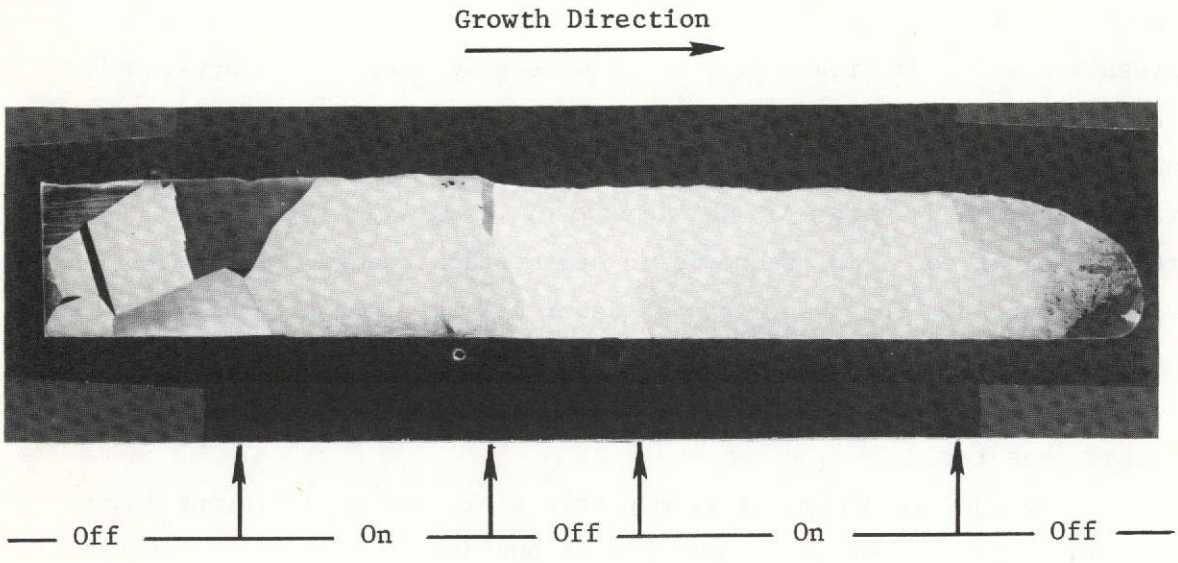

FIGURE 10. EFFECT OF MAGNETIC FIELD ON CRYSTAL GROWTH (INGOT 31012-16)

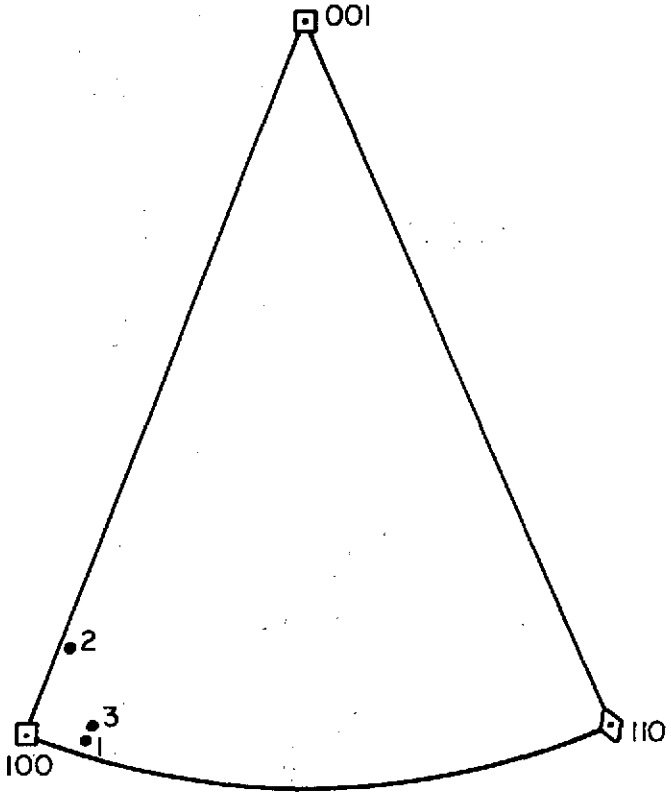

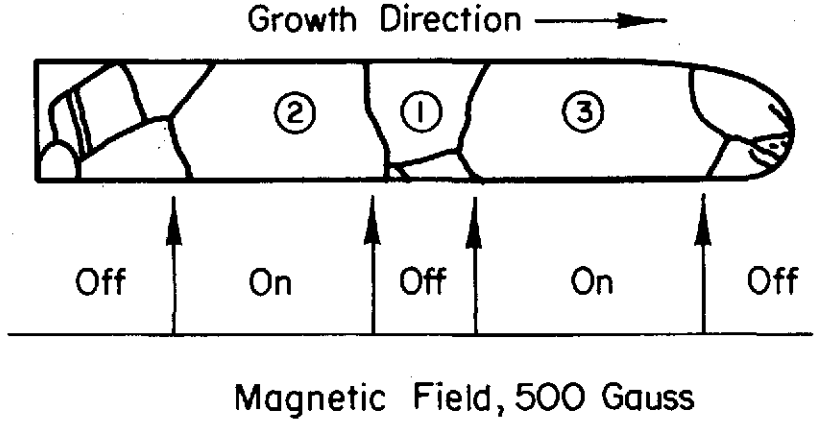

FIGURE 11. ORIENTATION OF GROWTH AXES ON STEREOGRAPHIC TRIANGLE FOR CRYSTALS 1, 2, AND 3 PRESENT IN INGOT 31012-16; POSITIONS OF CRYSTALS 1, 2, AND 3 IN INGOT

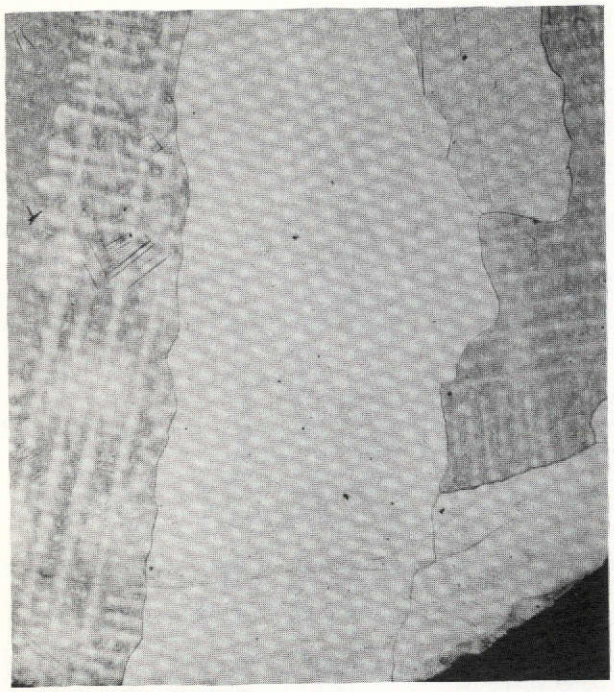

a. Ingot 31012-27, Magnetic Field 0, Cooling Rate 13 C/Min

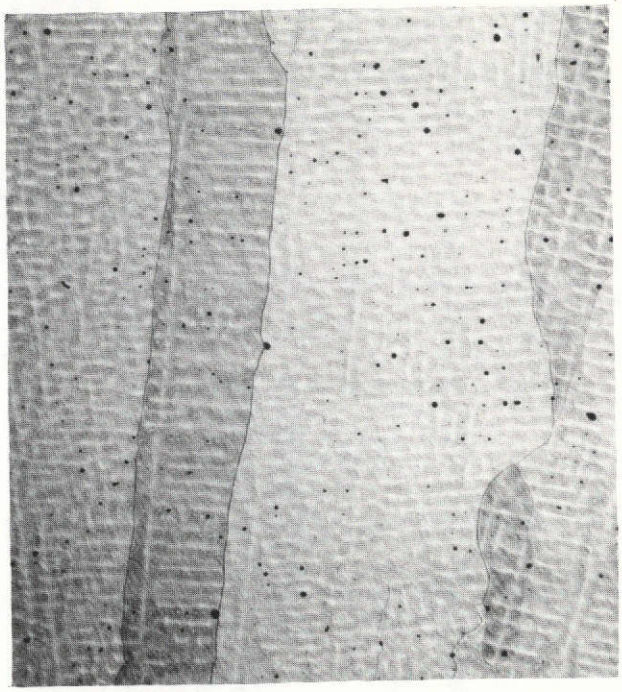

b. Ingot 31012-23, Magnetic Field 4000 Gauss, Cooling Rate 11 C/ Min

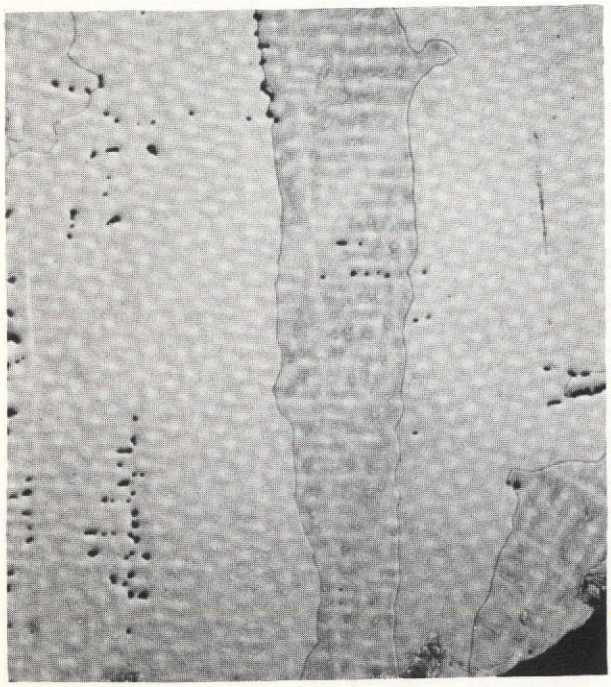

c. Ingot 31012-29, Magnetic Field 150 Gauss, Cooling Rate 7 C/ Min

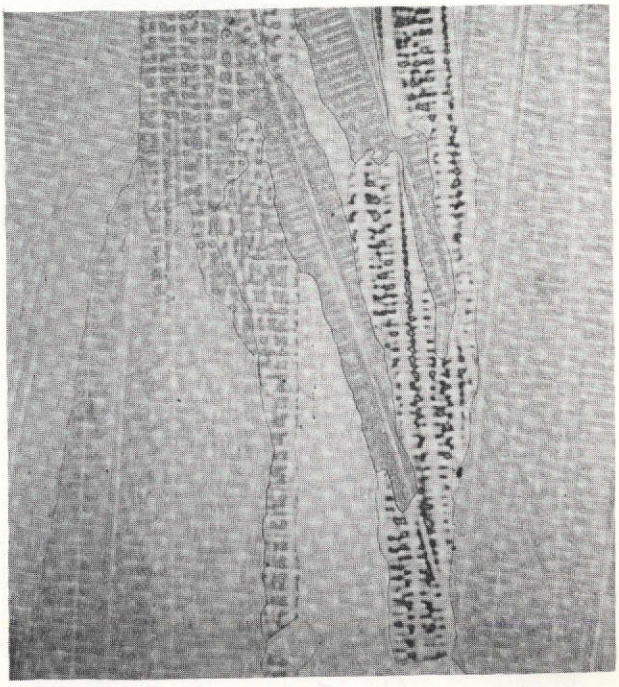

d. Ingot 31012-31, Magnetic Field 4000 Gauss, Cooling Rate 22 C/ Min

FIGURE 12. EFFECT OF MAGNETIC FIELD ON DENDRITIC GROWTH (20X)

have produced relatively fine oriented dendritic growth, even though the cooling rate was very slow. The finest dendritic structure was obtained in Ingot 31 (Figure 12d), which was frozen at a high rate in a 4000-gauss magnetic field.

Data upon which this report is based are recorded in Battelle Laboratory Record Book 31012, pages 1-35.

REFERENCES

(1) Tiller, W. A., Jackson, K. A., Rutter, J. W., and Chalmers, B., Acta Met., 1, 428 (1953).

(2) Mueller, A., and Wilhelm, M., Zeitschrift für Naturfarschung, 19a, 254 (1964).

(3) Utech, H. P., and Flemings, M. C., Crystal Growth, Ed. by H. S. Peiser, Pergamon Press, Oxford (1967), p. 651.

(4) Smith, V. G., Tiller, W. A., and Rutter, J. W., Can. J. Phys., 33, (1955) 723.

(5) Burton, J. A., Primm, R. C., and Slichter, W. P., J. Chem. Phys., 21, 1987 (1953).

(6) Yim, W. M., and Dismukes, J. P., Crystal Growth, Ed. by H. S. Peiser, Pergamon Press, Oxford (1967) p. 190.

(7) Hurle, D. T. J., ibid, p. 659.

(8) Cole, G. S., and Winegard, W. C., Canadian Met. Quart., 1, 29 (1962); J. Inst. of Metals, 93, 153 (1965).

(9) Wilcox, W. R., and Fullmer, C. D., J. Appl. Physics, 36, 2201 (1965).

(10) Mueller, A., and Wilhelm, M. Zeitschrift für Naturforschung, 19a, (2), 254 (1964).

(11) Utech, H. P., and Flemings, M. C., J. Appl. Physics, 37, 2021 (1966).

(12) Carruthers, J. R., and Winegard, W. C., Crystal Growth, Ed. by H. S. Peiser, Pergamon Press, Oxford, (1967) p. 695.

(13) Chandrasekhar, S., Hydrodynamics and Hydromagnetic Stability, Oxford University Press (1961).

(14) Cowling, T. G., Magnetohydrodynamics, Interscience (1957).

(15) Henderson, S. H., and Miller, R. I., "Analysis of Field Effects of Dense Liquid Materials", Final Report, NASA Contract No. NAS8-28664 (May 9, 1973).

(16) Turnbull, David., Trans. Met. Soc., AIME, 221, 422 (June, 1961).

(17) Cohen, M. H., and Turnbull, D., J. Chem. Phy., 31 (5), 1164 (November, 1959).

(18) Turnbull, D., and Cohen, M. H., J. Chem. Phys., 34 (1), 120 (January, 1961).

(19) Turnbull, D., and Cohen, M. H., "On the Free-Volume Model of the Liquid-Glass Transition", Tech. Report No. 24, Office of Naval Research (September, 1969).

(20) Andrews, K. W., et al., Proc. Roy. Soc. London, A177, 154 (1940-41).